

## Material Constants of a Constitutive Model Determination and Use

by

A. Varadarajan\*

and

C.S. Desai\*\*

### Introduction

In recent times, a number of constitutive models are proposed to characterize the stress-strain response of soils. These models usually involve a number of material constants and use of a number of advanced laboratory tests under various stress paths, often using multiaxial devices. However, a majority of geotechnical engineering laboratories are equipped with standard triaxial testing devices that allow testing of cylindrical specimens under a limited number of stress paths. In order to utilize such 'standard' testing facility for finding material constants for practical application, an attempt is made in this paper to evolve a methodology to identify the minimum number of standard tests for evaluation of the constants through a systematic process of analysis and verification. In addition, this study considers a number of special factors that influence the behaviour of sands.

The constitutive model using the recently proposed (Desai *et al.*, 1986) heirarchical approach is considered herein. The main attractive feature of this approach is that it allows the analyst to vary the complexity of the model and the related number of material constants, consistent with the practical requirement of a given problem. The potential application of such tailored models to various practical problems in sand medium is also discussed.

### Review

Many constitutive models have been proposed in the recent past to characterize the behaviour of soils. These include models based on non-linear elasticity, plasticity and endochronic theory. Since the main empha-

---

\*Professor, and Head, Dept. of Civil Engg., IIT, Delhi, India.

\*\*Regent's Professor, Dept. of Civil Eng. & Eng. Mech., University of Arizona, Tucson, AZ, USA.

sis here is on a plasticity based model, a brief review of relevant publications is provided below.

Classical plasticity models such as Tresca and von Mises were modified to account for frictional characteristics of soils; this resulted in the well-known Mohr-Coulomb and Drucker-Prager models. They can yield satisfactory predictions for some materials, under certain loading conditions and states; however, they are not able to capture fully certain special characteristics of soils such as volume changes under shear, stress path dependence and nonassociative characteristics.

The development of the critical state soil mechanics concept (Schofield and Worth, 1968) provided a rational basis for modelling of volume change behaviour and continuous yielding of soils. A similar formulation, known as cap models (DiMaggio and Sandler, 1971) has been often used to characterize behaviour of a number of geological materials. These models, however, do not fully represent factors such as wide range of stress paths, volume changes under shear, and stress-induced anisotropy. To allow for these aspects, several plasticity models have been proposed by combining isotropic and kinematic plastic hardening rules. They include two and multi-surface models (Lacey and Prevost, 1987) and bounding surface models (Dafalias and Herman, 1982). Desai and co-workers (Desai, 1980; Desai and Faruque, 1984; Desai and Salami, 1987; Desai *et al.*, 1986; Desai and Varadarajan, 1987; DiMaggio and Sandler, 1971; Frantzis-konis *et al.*, 1986; Hashmi, 1986 and Salami, 1986) have used generalized elastoplastic hardening theory to develop a class of constitutive models based on hierarchical approach to define the behaviour of various geologic materials.

### Scope

The objective of this paper is to develop a methodology to define the minimum number of tests required for finding constants for a general constitutive model (Desai *et al.*, 1986 and Desai and Varadarajan, 1987); in this paper attention is restricted to two versions of the model : (1)  $\delta_0$ —isotropic hardening with associative flow rule and (2)  $\delta_1$ —isotropic hardening with nonassociative flow rule. This model allows for defining the basic features of the behaviour of sands such as continuous yield, stress path dependency, volume change and nonassociative response.

In this paper, two new and additional factors related to the sand behaviour are considered. They are : (1) dependence of yielding on mean stress including high stress levels and (2) dependence of nonassociate response on stress path. Particular attention is devoted to the determination of material constants, the constants required to characterise various observed responses of sands, and the minimum number of tests required to evaluate

them. Potential application of the model to practical problems is also discussed.

Results of drained standard triaxial test on a dense sand, called Badarpur Sand, available at a stone crusher plant in the vicinity of Badarpur town near Delhi, India, are used to evaluate various conditions related to the proposed model.

### Proposed Model and Determination of Material Constants

The basic concept, theoretical development and application of the proposed model are given previously (Desai *et al.*, 1986). The distinguishing feature of this model is that a unified or hierarchical approach is adopted in the development to systematically include responses of progressive complexities such as isotropic hardening with associative flow rule, isotropic hardening with nonassociative flow rule, anisotropic hardening and strain softening. This approach enables simplification in the determination of material constants from the laboratory tests and the number of constants as well.

The model possesses a number of advantages over the two and multi-surface models such as critical state (Schofield and Wroth, 1968), cap (DiMaggio and Sandler, 1971) and that proposed by Lade (1977). For instance, the continuous yield surface in this model avoids the discontinuity at the intersection of the cap and failure or critical state surface, and thereby eliminates the resultant computational problems.

A number of important basic features of the model are used herein to define the behaviour of the dense sand. The model is further extended to incorporate some special aspects of the responses to the sand. These are briefly discussed in the following :

The continuous yielding and ultimate yield behaviour is given by a compact and specialized form of the general polynomial representation (Desai, 1980 and Desai *et al.*, 1986) as

$$F = J_{2D} - \left( \frac{-\alpha}{\alpha_0^{n-2}} J_1^n + \gamma J_1^2 \right) (1 - \beta S_r)^m = J_{2D} - F_b F_s = 0 \quad (1)$$

where  $J_{2D}$  is second invariant of the deviatoric stress tensor,  $S_{ij}$ , of the total stress tensor,  $\sigma_{ij}$ ,  $S_r$  is stress ratio equal to  $J_{3D}^{1/3} / J_{2D}^{1/2}$ ,  $J_{3D}$  is third invariant of  $S_{ij}$ , and  $\alpha$ ,  $n$ ,  $\gamma$ ,  $\beta$  and  $m$  are the response functions.  $F_b$  is component function and  $F_s$  is shape function. The value of the normalizing constant,  $\alpha_0$ , is equal to 1.0 kPa. Different  $S_r$  values designate different stress paths such as  $S_r = 1$ , compression path ( $\sigma_1 > \sigma_2 = \sigma_3$ ) and

$S_r = -1$ , extension path ( $\sigma_1 = \sigma_2 > \sigma_3$ ), where  $\sigma_1$ ,  $\sigma_2$  and  $\sigma_3$  are major intermediate and minor principal stresses.

Plots of  $F$  for the Badarpur Sand in the  $J_1 - \sqrt{J_2 D}$  space are shown in Fig. 1(a) for a typical stress path, and in Fig. 1(b) the same on the octahedral plane. The function  $F$  is continuous in the stress space with the final curve representing the ultimate behaviour. The component function  $F_b$ , (Eq. 1) defines  $F$  in  $J_1 - \sqrt{J_2 D}$  space, Fig. 1(a), and the component  $F_s$  denotes  $F$  in the octahedral plane, Fig. 1(b).

### *Straight Ultimate Envelope*

The function  $F$  at ultimate state (where  $\alpha = 0$ ) is given by

$$F = J_{2D} - \gamma J_1^2 (1 - \beta S_r)^m = 0$$

or

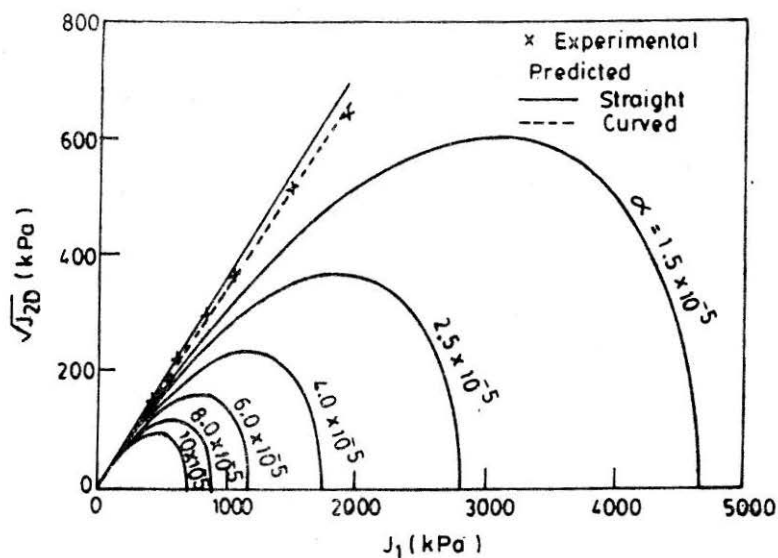
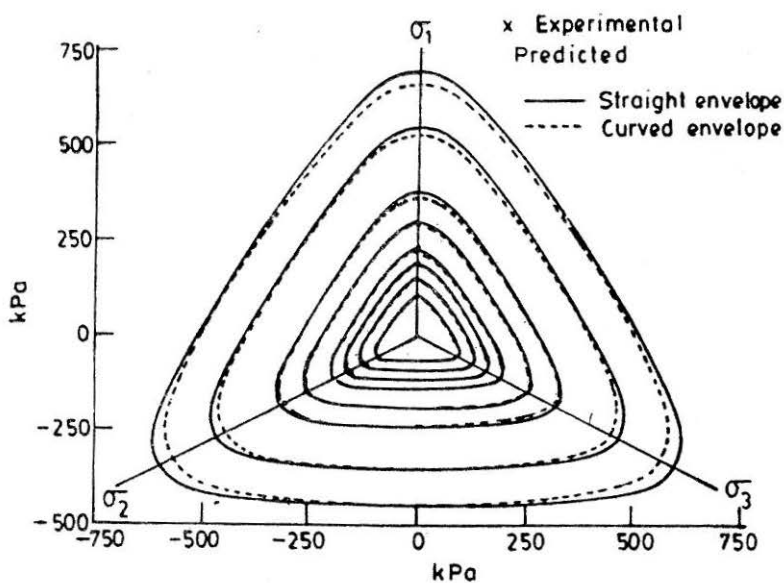
$$\sqrt{J_{2D}} = \sqrt{\gamma} J_1 (1 - \beta S_r)^{m/2} \quad (2)$$

Equation (2) represents the locus of the stress states asymptotic to the observed stress-strain curves from different stress paths. The normally adopted failure ( $F$ ) and critical states ( $CS$ ) are usually below this state or may coincide with it (Fig. 2). With  $m$ ,  $\gamma$  and  $\beta$  as constants, Eq. (2) gives a straight line envelope of the ultimate state. This envelope can be applicable to the working stress range of many practical problems such as footing foundation, earth backfill in retaining structures and small embankments.

Ultimate values of constants  $m$ ,  $\gamma$  and  $\beta$  are found by curve fitting the ultimate envelopes (Fig. 1). The value of  $m$  for many geologic materials is found to be  $-0.50$ . To find the constants  $\gamma$  and  $\beta$  in Eq. 2, at least two tests with different stress paths (i.e. with two  $S_r$  values) are essential. It is important to note that stress paths generated by various combinations of  $\sigma_1$  and  $\sigma_3$  but with the same  $S_r$  value ( $\sigma_1 > \sigma_2 = \sigma_3$  for example) may not fulfil the above condition.

In many standard soil testing laboratories, tests under only one stress path, which is usually the conventional triaxial compression (CTC) path, ( $\sigma_1 > \sigma_2 = \sigma_3$ ), are conducted using the standard strain controlled triaxial equipment. In such cases, if it is possible to assume that the angle of shearing resistance under compression and extension in the Mohr-Coulomb space is the same, that is,  $\phi_C = \phi_E$ , then a point corresponding to the second stress path test (extension here) can be estimated using the relation

$$-(\sigma_1 - \sigma_3) = (\sigma_1 + \sigma_3) \sin \phi_E \quad (3)$$


 (a) In  $J_1 - \sqrt{J_2 D}$  space: Compression path ( $Sr = -1.0$ )


(b) In octahedral planes

 FIGURE 1 Plots of  $F$  in  $J_1 - \sqrt{J_2 D}$  Spaces for Badarpur Sand

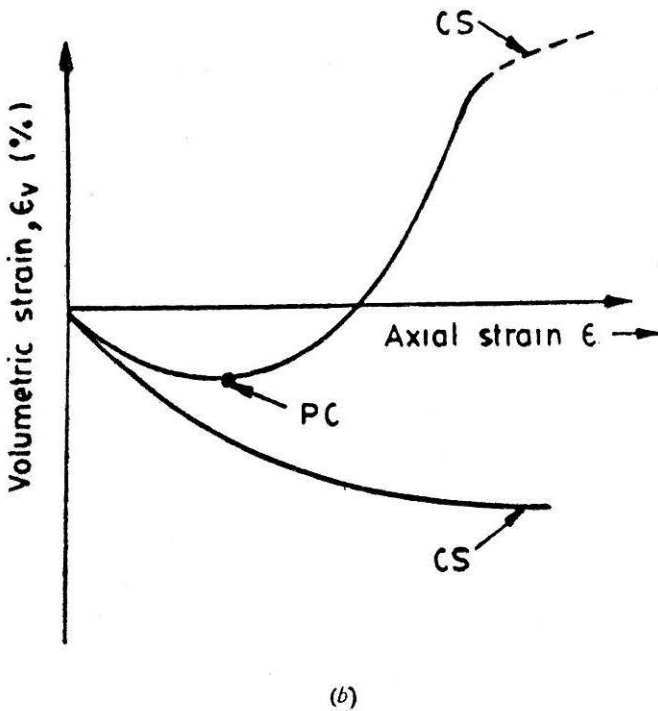
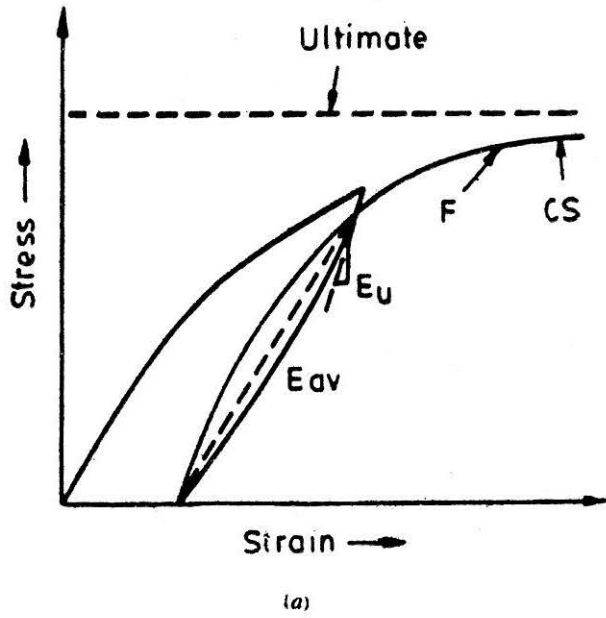


FIGURE 2 Ultimate, Phase Change and Critical States

*Curved Ultimate Envelope*

In certain practical problems such as high earth dams and heavily loaded foundations, the mean stress values are high and in such cases, the ultimate envelope as well as the yielding will be stress dependent. To allow for this aspect, stress dependent yield behaviour, as proposed by Desai and Varadarajan (1987) for rock salt, is adopted here. For this case,

$$F_s = ((\exp \frac{\beta_1}{\beta_0} J_1) - \beta S_r)^n \quad (4)$$

where  $\beta$  and  $\beta_1$  are constants. The value of normalizing constant  $\beta_0$  is equal to 1.0 kPa. With this variation, the shape of yield surface in the octahedral plane is triangular with smooth corners at low stress, and at higher stress the corners become increasingly rounded and the sides assume convex shapes (Fig. 1b). At very large values of  $J_1$ , the differences in the values of  $\sqrt{J_2 D}$  for different stress paths (compression, extension and simple shear) tend to reduce, leading to a nearly circular surface in the octahedral plane. Ultimate values of constants  $\gamma$ ,  $\beta$  and  $\beta_1$  are found by curve fitting. The procedure for determination of these constants is described in detail in Desai and Varadarajan (1987), while a brief discussion is presented here.

The values of  $\beta$  and  $\beta_1$  are determined first by using the values of  $\sqrt{J_2 D}$  for compression (C) and extension (E) at the same  $J_1$  values. This leads to

$$-\beta e^{-J_1 \beta_1} = r^* \quad (5)$$

where  $r^* = (r^4 - 1)/(r^4 + 1)$ ,  $r = (\sqrt{J_2 D})_C / (\sqrt{J_2 D})_E$ . Taking logarithm of both sides,  $\ln(-\beta) - J_1 \beta_1 = \ln r^*$ . From a straight line plot of  $\ln r^*$  vs.  $-J_1$  from experimental results, the values of  $\beta$  and  $\beta_1$  are determined.

For determination of these constants, a minimum of two points with two  $J_1$  values and corresponding  $r^*$  values are required. For this purpose, at least four test results with two stress paths (compression and extension in this case) at two  $J_1$  values are required.

At the ultimate condition, Eqs. 1 and 4 give

$$J_2 D F_s = \gamma J_1^2 \quad (6)$$

or  $F_1 = J_1^2$  where  $F_1 = J_2 D F_s$ . The value of  $\gamma$  is determined by fitting a straight line for various experimental values of  $F_1$  and  $J_1$ . To find  $\gamma$ , the same number of tests indicated above are sufficient.

### Phase Change or Transition Point

Parameter  $n$  represents the phase change point indicating transition from compressive to dilation volume change (Fig. 2). The value of  $n$  is determined from the state of stress at which contractive volume change transits to dilation in the axial strain vs volumetric strain plot. Thus, use of  $\frac{\partial F}{\partial J_1} = 0$ , (neglecting  $\frac{\partial F_s}{\partial J_1}$ , which is very small in case curved envelope is used) leads to

$$1 - \frac{2}{n} = \frac{J_{2D}/J_1^2}{F_s \gamma} \quad (7)$$

at the phase change point, and allows computation of  $n$ . For finding the value of  $n$ , at least one test is required.

### Hardening Function

The hardening behaviour is included in the model by using a growth function,  $\alpha$ . Among the different forms of  $\alpha$  that can be developed depending upon the observed behaviour, a simple form is used here as

$$\alpha = \frac{a_1}{\xi^{\eta_1}} \quad (8)$$

where  $a_1$  and  $\eta_1$  are hardening constants and  $\xi = \int (d\epsilon_{ij}^p d\epsilon_{ij}^p)^{1/2} =$  trajectory of total plastic strain.

Figure 3, shows plot of transformed form of Eq. 8, in terms of  $-\ln(\xi)$  vs.  $\ln(\alpha)$  from results of tests along various stress paths for the Badarpur Sand. The values of  $a_1$  and  $\eta_1$  are obtained by fitting an average straight line. Approximate values of these constants can be determined even from results of single test.

### Associative Flow Rule

The proposed model, (Eq. 1), is based on the assumption of initially isotropic material and isotropic hardening with associative response in which yield function  $F$  acts as the plastic potential function. In this form, the model predicts high volume expansion in relation to the experimental values, particularly at high shear stress level (for example, Fig. 4). The model, therefore, can be employed for field problems where low shear stress mobilisation is anticipated; for example, footing foundation with the usually adopted factor of safety of two or more against failure.

### Nonassociative Flow Rule

To allow for realistic prediction of volume changes at higher shear



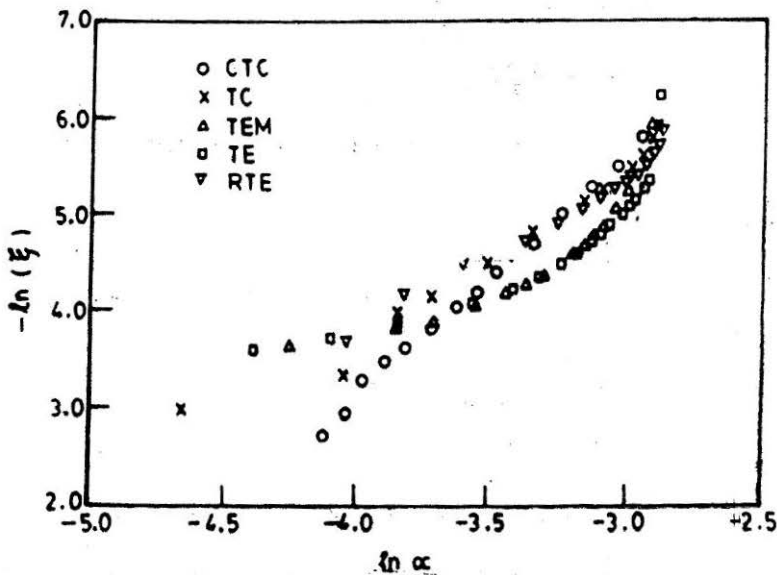


FIGURE 3 Determination of  $\alpha_1$  and  $\eta_1$  for Badarpur Sand

stresses developed in such field problems as embankments, earth backfills and underground openings in cohesionless soils it is necessary to develop a plastic potential function  $Q$ , and apply nonassociative plasticity. This can be achieved by correcting or controlling the yield function  $F$  to  $\bar{F}$  as proposed previously, (Desai and Faruque, 1984; Frantziskonis, *et al.*, 1986). In this case, the plastic potential function  $Q = F$  is formulated by correcting the growth function  $a$  in Eq. (1) as  $\alpha_Q$  and is expressed as

$$\alpha_Q = a + \kappa (a_I - a) (1 - r_v) \quad (9)$$

where  $r_v = \xi_v/\xi$  and  $\xi_v$  is the volumetric part of  $\xi$ ,  $\kappa$  is the material parameter and  $a_I$  is the value of  $a$  at the initiation of nonassociative behaviour, usually assumed to occur at the end of hydrostatic compression.

In Eq. (9), the value of  $\kappa$  is assumed to apply to all stress paths. But, a more general case is the one in which the nonassociative behaviour is influenced by the stress path. To account for this aspect, Eq. 9, is modified in this paper as

$$\alpha_Q = a + (\kappa_1 + \kappa_2 S_r) (a_I - a) (1 - r_v) \quad (10)$$

where  $\kappa_1$  and  $\kappa_2$  are material constants. These constants are found from the observed volume trice behaviour near the ultimate state. At the ultimate states  $a = 0$  and from Eq. 1,

$$\alpha_Q = (\kappa_1 + \kappa_2 S_r) a_I (1 - r_v) \quad (11)$$

From the flow rule of plastic loading,

$$d\epsilon_v^p = 3\lambda \frac{\partial Q}{\partial J_1} \quad (12)$$

where  $\epsilon_v^p$  is the volumetric plastic strain  $\epsilon_v^p = \epsilon_{ii}^p$  (summation of indices implied). Also,

$$d\epsilon_{11}^p = \lambda \frac{\partial Q}{\partial \sigma_{11}} \quad (13)$$

From Eqs. (12) and (13),

$$\frac{d\epsilon_v^p}{d\epsilon_{11}^p} = \frac{3\partial Q/\partial J_1}{\partial Q/\partial \sigma_{11}} \quad (14)$$

The ratio of  $d\epsilon_v^p / d\epsilon_{11}^p$  can be obtained as the slope of the observed  $\epsilon_v^p$  vs  $\epsilon_{11}^p$  response by choosing a point in the ultimate state. Next, the value of  $\alpha_Q$ , which is represented by the right hand side of Eq. can be found since the left hand side is now known. The constants  $\kappa_1$  and  $\kappa_2$  can then be determined using Eq. 11. To find these constants, at least two tests with two different stress paths are required. For finding stress path independent  $\kappa$  value in Eq. 9, one test is sufficient.

#### *Elastic Behaviour*

The Young's modulus,  $E$ , and the Poisson's ratio,  $\mu$ , are commonly evaluated using unloading-reloading response. In some cases, the (average) slope of the initial portions of the stress-strain curves and the axial strain vs volumetric strain curves of CTC tests are used to find approximate values of  $E$  and  $\mu$ .

#### *Material Constants and Minimum Tests*

Table 1, presents the summary of various characteristics of the constitutive model, the number of material constants (excluding the elastic constants) and the minimum number of tests. To allow for the most general case; i.e., curved envelope with stress path dependent nonassociative response, eight constants are required for the plastic hardening. The minimum number of tests required for this case is four.

To represent the simplest case; i.e., straight envelope with associative behaviour, only five constants are necessary to describe plastic hardening. These can be determined even with one CTC test. Thus, the characteristics of the model can be varied by changing the number of constants to suit the

TABLE 1  
Material Parameters and Minimum Number of Tests for Various Cases

Type of envelope	Associative/ Nonassociative	Ultimate		Constants		Phase change	Hardening		Nonassociative		Total No. of constants	Minimum no. of tests	
		m	$\gamma$	B	$B_1$	n	$a_1$	$n_1$	$K_1$	$K_2$			
		$\phi_E = \phi_C$	Associative	-0.50	✓	✓	NA	✓	✓	✓			NA
	Nonassociative stress path independent	-0.50	✓	✓	NA	✓	✓	✓	✓	NA	NA	6	
Straight Envelope	Nonassociative stress path dependent	-0.50	✓	✓	NA	✓	✓	✓	NA	✓	✓	7	paths
	$\phi_C = \phi_E$	Associative	-0.50	✓	✓	NA	✓	✓	✓	NA	NA	NA	5
	Nonassociative stress path independent	-0.50	✓	✓	NA	✓	✓	✓	✓	NA	✓	6	CTC Test
Curved Envelope	Associative	-0.50	✓	✓	✓	✓	✓	✓	NA	NA	NA	6	Four
	Nonassociative stress path independent	-0.50	✓	✓	✓	✓	✓	✓	✓	NA	NA	7	Tests with
	Nonassociative stress path dependent	-0.50	✓	✓	✓	✓	✓	✓	NA	✓	✓	8	Two Stress Path

✓ = Required, NA = Not Applicable.

requirement of the field problem to be analysed. Also, the standard experimental set-up commonly available in a typical soil engineering laboratory can be utilized to estimate the constants. However, it must be pointed out that to find improved values of the constants, greater number of tests under different stress paths may be used.

It is important to note that the constants in the proposed model have physical meanings and they are related to specific and strategic states during the deformation process.

### Laboratory Tests

To examine various characteristics of the proposed model and the effect of reducing the number of tests for finding the material constants, the experimental results of a dense sand were used.

### Soil

The Badarpur Sand, which consists of brick red angular quartz particles was used. It has particle sizes ranging from 0.06 mm to 2.00mm and is uniformly graded (uniformity coefficient = 1.72). The specific gravity of solids is 2.66.

### Tests

A number of drained triaxial tests were conducted using standard triaxial device six different stress paths : one hydrostatic compression (HC); three conventional triaxial compression (CTC) tests with initial confining pressures,  $\sigma_0 = 137.3, 205.80$  and  $274.6$  kPa; three triaxial compression (TC) tests with the above confining pressures; one reduced extension test (RTE) with  $\sigma_0 = 137.3$  kPa; one triaxial extension test with  $\sigma = 137.3$  kPa (TE); and one test called triaxial extension modified (TEM), in which  $(\sigma_1 + \sigma_3)/2$  remained constant with  $\sigma_0 = 137.3$  kPa.

Saturated specimens of size 3.81 cm dia and 7.62 cm long and relative density  $D_r = 89\%$  were used for the testing. A uniform procedure of tamping was adopted to achieve the same initial density. Frictionless end platens were used to reduce the end friction. The cell pressure was applied by a self-compensating mercury pot system. Stress-controlled loading was applied through piston using a loading frame consisting of hanger and lever system. A proving ring was used to measure the axial load. Volume changes of specimens were measured using a small burette having an accuracy of 0.01 cc. Membrane penetration effect was studied using the procedure described by Roscoe *et al.* (1963). The volume change due to membrane penetration was found to be negligible within the range of the pressures used, and hence, it was not included. For (extension)

tests requiring lateral stress greater than the vertical stress, a triaxial cell with a specific loading ram of 3.81 cm diameter was used.

Triaxial tests were conducted by applying small increments of loading to follow the desired stress paths. Area corrections for specimens, load increment to be applied on the piston and the change in cell pressure were all calculated for every load step using a programmable calculator. The complete details of the equipment and testing procedure are given by Mishra (1981).

### Material Constants

Table 2, shows the constants found for the Badarpur Sand. The ultimate constants were determined using all the test results, but the hardening parameters were determined using the results of five stress path tests at  $\sigma_0 = 137.3 \text{ kPa}$ . The characteristics of the proposed model were first studied. They consisted of investigating the effects of the nature of ultimate envelope and the use of various nonassociative constants. The envelope was treated as a curve (CASE A) and as a straight line (CASE B). The nonassociative constant was taken as an average value,  $\kappa$  and as stress-path dependent constants  $\kappa_1$  and  $\kappa_2$  (Eq. 10).

Secondly, the effect of number of tests on the constants was investigated by using : (i) two tests, one CTC ( $\sigma_0 = 137.3 \text{ kPa}$ ) and one TE Test ( $\sigma_0 = 137.3 \text{ kPa}$ ) (Case C) and (ii) one CTC test only ( $\sigma_0 = 137.3 \text{ kPa}$ ) (Case D). For both the cases, straight envelope was adopted. The parameters for these two cases are also shown in Table 2. It can be seen that most of the constants for Cases C and D (refer to values in Table 2) are not much different from those in Case B which uses a greater number of tests; only in the case of  $\kappa$ , there is about 30 percent difference between Cases D and B. The differences in material constants noted herein, however, the same for all sands.

It must be mentioned that this model requires equal or smaller number of tests than those required for finding constants for the available nonlinear elastic (hyperbola, spline, etc.) and other plasticity models of comparable quality.

### Comparisons

The various characteristics of the proposed model are compared herein with the experimental results. For this purpose, the normality rule

$$d\epsilon_{ij}^p = \lambda \frac{\partial \sigma}{\partial \sigma_{ij}} \quad (15)$$

where  $\lambda$  = scalar proportionality parameter, and the consistency condition  $dF = 0$  are used to derive the incremental stress-strain relations as

TABLE 2  
Material Constants for Badarpur Sand

		Curved Envelope	Straight Envelope	Straight Envelope	
		Case A	Case B	Case C	Case D
Tests Used		Nine Tests for Ultimate and Five Tests for Others Plasticity Parameters		Two Tests One CTC and One TE Test	One CTC Test ( $\phi_C = \phi_E$ )
150,000 kPa, 0.30					
Elasticity	$E, \mu,$				
$m = -0.50$					
Ultimate	$\gamma$	0.07020	0.07022	0.06981	0.06190
	$\beta$	-0.6900	-0.70169	-0.66408	-0.73586
	$\beta_1$	0.00003	—	—	—
	$\beta_0$	0.0 kPa	—	—	—
Phase Change	$n$	3.00	3.00	2.8	2.9
Hardening	$a_1$	0.003166	0.003850	0.003664	0.0031310
	$\eta_1$	0.49317	0.45000	0.50480	0.50400
$a_0 = 1.0 \text{ kPa}$					
Nonassociative	$\kappa_1$	0.402	0.400	0.420	*
	$\kappa_2$	0.100	0.101	0.110	*
	$\kappa$	—	0.400		0.271

\*Insufficient test to find two constants

$$\{d\sigma\} = [C^{ep}] \{d\epsilon\} \quad (16)$$

where  $\{d\sigma\}$  and  $\{d\epsilon\}$  are vectors of incremental stress and strain component and  $[C^{ep}]$  is the constitutive matrix expressed in terms of the material constants. In the case of the associative plasticity, the function  $Q = F$  is used.

#### Ultimate Envelope Comparison

Figures 1(a) and 1(b) show the comparisons of the ultimate stresses in the  $J_1 - \sqrt{J_2 D}$  space and octahedral planes with the curved envelope and

straight envelope. The curved envelope shows improved agreement with the experimental results, particularly at high stress levels, as compared to the one with straight envelope with two parameters. At elevated stress levels such as the stress in an earth dam of height 80m with  $J_1$  of the order of 3600 kPa, the curvature is likely to be very significant, and it may become necessary to adopt the curved envelope.

### *Hardening Behaviour Comparison*

The hardening behaviour of the model is compared with the experimental results in two sets : SET I, by varying the number of constants and SET II by varying the number of tests to find the constants. In SET I, the comparison is performed as follows :

*Case I*—Straight envelope with associative flow rule and nonassociative flow rule [5 and 6 or 7 constants, Table 1, Table 2 (Case B)].

*Case II*—Straight envelope with one and two nonassociative constants [6 and 7 parameters, Table 1, Table 2].

*Case III*—Straight and curved envelopes with two nonassociative constants [7 and 8 parameters, Table 1, Table 2, (Case A and Case B)].

In Set II the comparisons are made with two cases :

*Case IV*—Constants found from five tests and two tests (Table 2, Case B and Case C).

*Case V*—Constants found from five tests and one test (Table 2, Case B and Case D).

In this set, the straight line envelope was used. In Case V one nonassociative parameter was adopted.

### *Set I*

#### **Case I**

Figures 4-6 present the comparison of observed and predicted behaviour of the sand with associative and nonassociative models for CTC, TC and TEM stress paths (with  $\sigma_0 = 137.3$  kPa). Both the models give satisfactory predictions with respect to volume change at low shear stress levels ( $< 70\%$  of total shear stress). But, at higher shear stress levels, only non-associative model predicts satisfactory volume change behaviour.

#### **Case II**

In Figs. 4 and 6 are presented the effect of using two stress path dependent nonassociative parameters. It may be noted that the use of the two

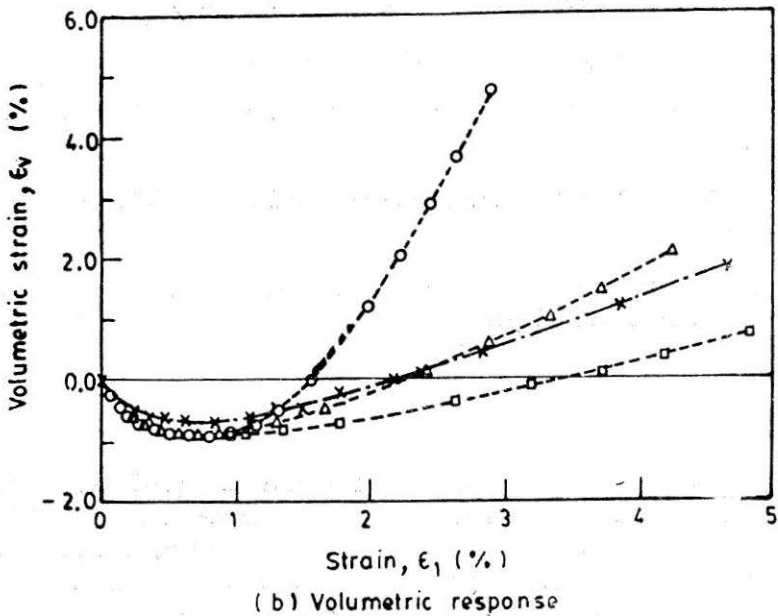
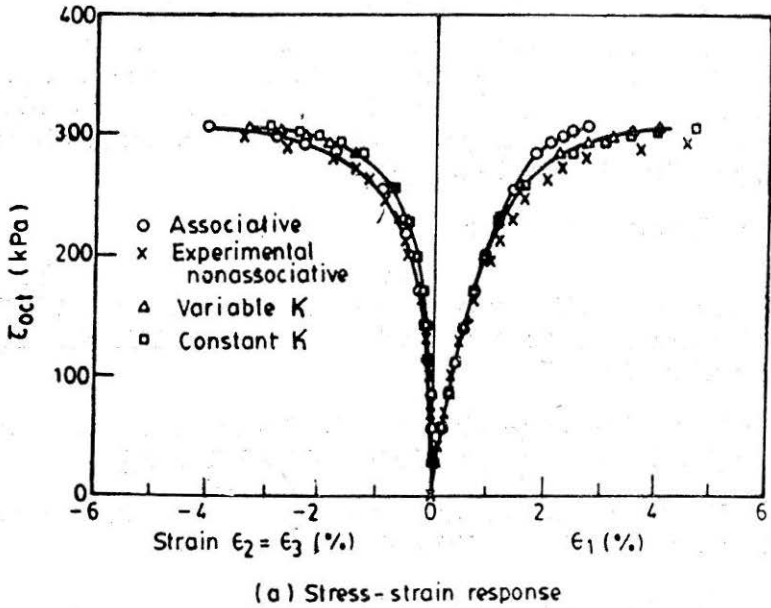


FIGURE 4 Comparison Between Predictions and Observations for CTC TEST  $\sigma_0 = 137.3$  kPa, Badarpur Sand

constants shows improved prediction in the volume change behaviour and it appears, therefore, appropriate to adopt stress path dependent non-associative behaviour.



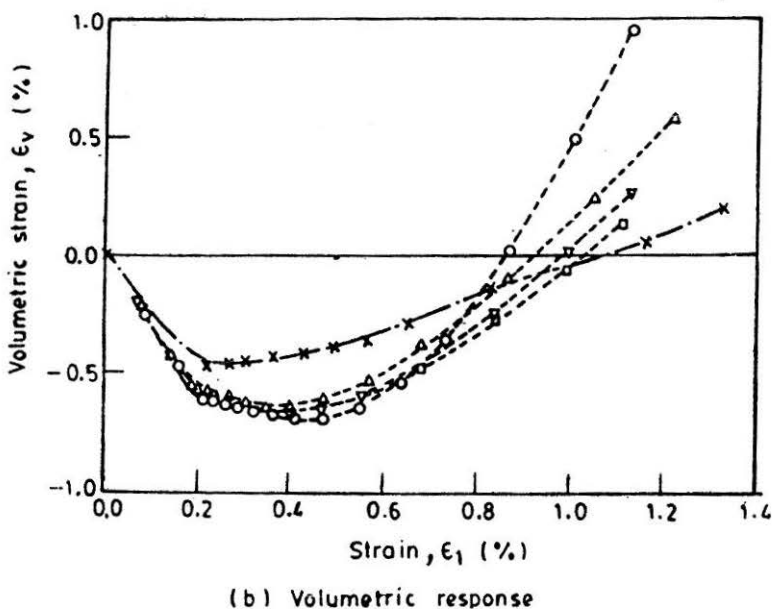
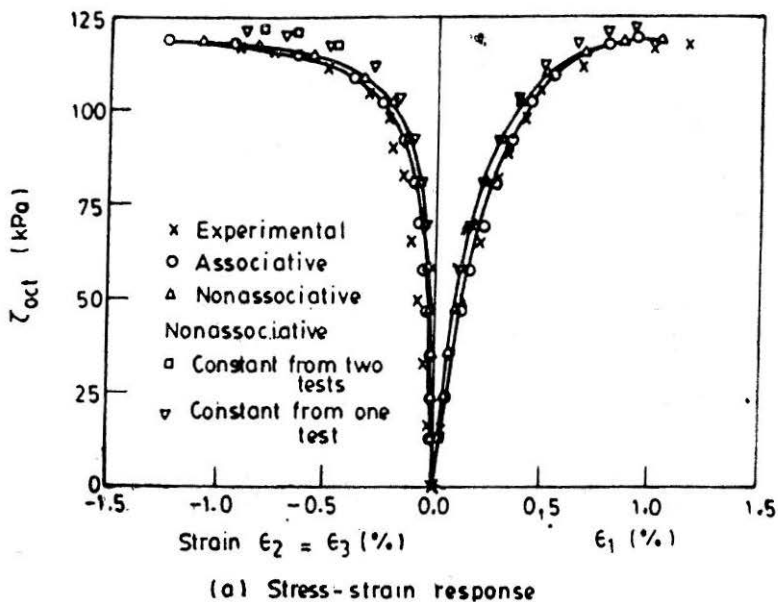
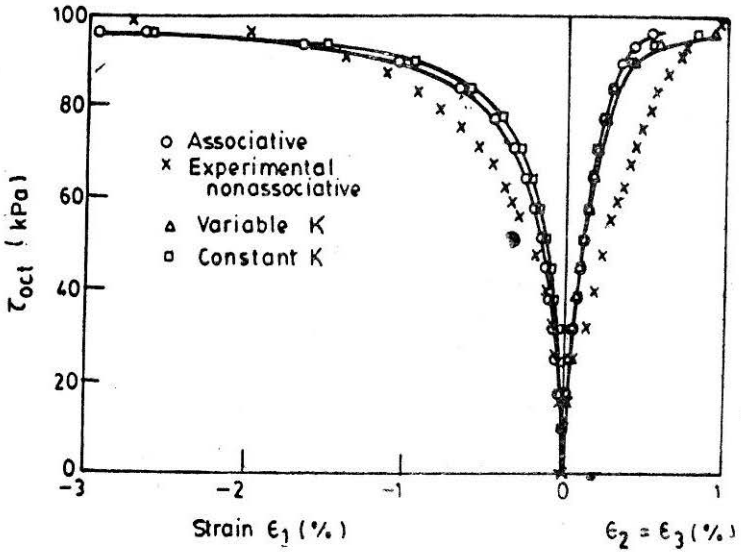


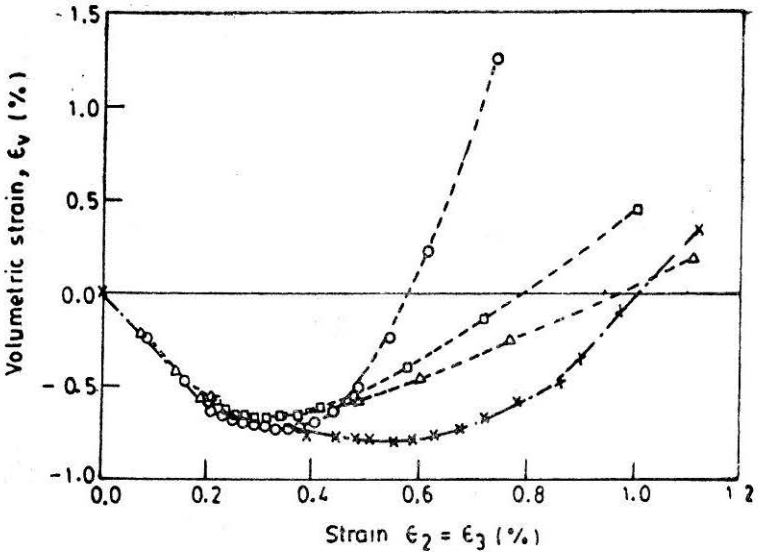
FIGURE 5 Comparison Between Predictions and Observations from TC TEST,  $\sigma_0 = 137.3$  kPa, Badarpur Sand

Case III

The comparison of predictions with straight and curved envelopes is shown in Fig. 7 for CTC path ( $\sigma_0 = 274.6$  kPa). The stress-strain as well



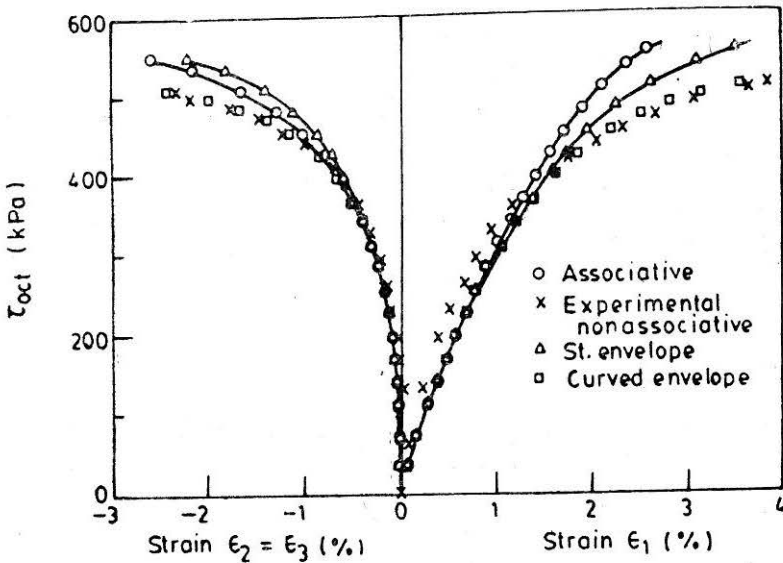
(a) Stress - strain response



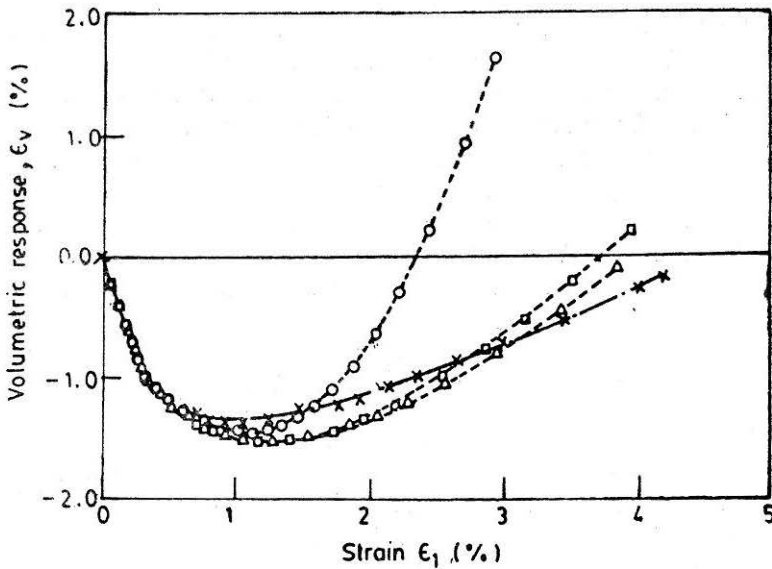
(b) Volumetric response

FIGURE 6 Comparison Between Predictions and Observations for TEM TEST,  $\sigma_o = 137.3$  kPa, Badarpur Sand

as volume change are closer to the experimental results for curved envelope with nonassociative flow rule.



(a) Stress-strain response



(b) Volumetric response

FIGURE 7 Comparisons Between Predictions and Observations for CTC Tess,  $\sigma_o = 274.6$  kPa, Badarpur Sand

It must be pointed out that this experimental result was not used for finding the constants.

## Set II

### Case IV and Case V

Figure 5 presents the predictions for TC path by using the constants from reduced number of tests. It must be noted that for finding the constants for Cases C and D (Table 2), this test was not used. It can be seen that the predictions with constants from only two tests (Case C) show satisfactory correlation with the observed behaviour. The prediction with constants from only one set with  $\phi_C = \phi_E$  (Case D) is not that satisfactory, but shows reasonable correlation with the observed behaviour.

### Conclusions and Potential Use

It is shown, from an analysis involving back predictions of observed stress-strain behaviour of a sand, that material for a general model capable of accounting for a number of important behavioural aspects can be estimated from a set of standard triaxial test. The number of plasticity constants for the simple (straight ultimate envelope) version, namely five (with  $m = -0.5$  and two elastic constants), is equal to or smaller than those involved in other elasticity and plasticity models often used in geotechnical engineering. At the same time, the model is capable of allowing for factors such as volume change, nonassociative response and stress path dependency. Other important advantages of the model are : (1) the constants have physical meanings that are related to specific physical states during deformation, (2) the procedure for finding constants is relatively straightforward, (3) hardening is dependent on total (volumetric plus deviatoric) plastic strain trajectory instead of only volumetric as in critical state and cap models, (4) additional complexities such as curved envelope and dependence of nonassociative behaviour on stress path can be conveniently introduced with additional constants, and it can be easily implemented in nonlinear solution (finite element) procedures; here, because of the continuous nature of yield surfaces, the computational difficulties with multi-surface model are avoided, Hashmi (1986).

The model possesses potential applications for a number of geotechnical problems. The simple model with straight ultimate envelope and  $k = \text{constant}$  can be used for shallow foundations, slopes and retaining walls founded in sands. The curved envelope model can be used for structures such as dams and piles involving higher mean stress.

At the present time, a large number of constitutive models are developed and proposed, often with a large number of constants without specific physical meanings. From the viewpoint of the user, it is difficult to make a judgement as to how to decide on adopting such models. This paper presents a systematic procedure towards development of a methodology for a given model to arrive at minimum number of constants and standard

tests required for their estimation. Thus, the results can constitute a step towards utilization of constitutive models for practical use.

## REFERENCES

- DAFALIAS, Y.F. and HERMAN, L.R. (1982), "Bounding Surface Formulation for Soil Plasticity", *Soil Mechanics, Transient and Cyclic Loads*, Ed. by G.N. Pande and O.C. Zienkiewicz, Wiley, pp. 253-282.
- DESAI, C.S. (1980), "A General Basis for Yield, Failure and Potential Functions in Plasticity", *Int. J. Num. Analyt. Meth. in Geomech.*, Vol. 4, pp. 361-375.
- DESAI, C.S. and FARUQUE, M.O. (1984), "A Constitutive Model for (Geologic) Materials", *J. of Eng. Mech. Div., ASCE*, Vol. 110, pp. 1391-1408.
- DESAI, C.S. and SALAMI, M.R. (1987), "Constitutive Model Including Testing for Soft Rock", *Int. J. of Rock Mech. and Min. Sc.*, Vol. 24, pp. 299-307.
- DESAI, C.S., SOMASUNDARAM, S. and FRANTZISKONIS, G. (1986), "A Hierarchical Approach for Constitutive Modelling of Geologic Materials", *Int. J. Num. Analyt. Meth. in Geomech.*, Vol. 10, No. 3.
- DESAI, C.S. and VARADARAJAN, A. (1987), "A Constitutive Model for Short Term Behaviour of Rock Salt", *J. of Geophysical Research*, Oct.
- DIMAGGIO, F.L. and SANDLER, I.S. (1971), "Material Model for Granular Soil", *J. of Eng. Mech. Div., AISC*, Vol. 97, pp. 935-950.
- FRANTZISKONIS, G., DESAI, C.S. and SOMASUNDARAM, S. (1986), "Constitutive Model for Nonassociative Behaviour", *J. of Eng. Mech. Div., ASCE*, Vol. 112, No. 9, pp. 932-946.
- HASHMI, Q. (1986), "Nonassociative Plasticity Model for Cohesionless Materials and Its Implementation in Soil-Structure Interaction", *Ph. D. Dissertation*, The University of Arizona, Tucson, AZ, U.S.A.
- LACEY, S.J. and PREVOST, J.H. (1987), "Constitutive Model for Geomaterials", *Constitutive Laws for Engg. Materials: Theory and Application*, Ed. C.S. Desai et al., Elsevier, pp. 149-160.
- LADE, P.V. (1977), "Elastic-Plastic Stresses-Strain Theory for Cohesionless Soil with Curved Yield Surfaces", *Int. J. Solids and Struct.*, Vol. 13, pp. 1019-1035.
- MISHRA, S.S. (1981), "Effect of Stress Path on the Stress-Strain-Volume Change Behaviour of Some Granular Soils", *Ph. D. Thesis*, Indian Institute of Technology, Delhi, India.
- MROZ, Z. and PIETRUSZCZAK, S. (1983), "Constitutive Model for Sand with Anisotropic Hardening Rule", *Int. J. Num. Analyt. Method in Geomech.*, Vol. 7, pp. 305-320.
- ROSCOE, K.H., SCHOFIELD, A.N. and THURIARAJAH, A. (1963), "An Evaluation of Test Data for Selecting Yield Criterion for Soils", *Special Technical Publication No. 361*, ASTM, pp. 111-133.
- SALAMI, M.R. (1986), "Constitutive Modelling of Concrete and Rock under Multiaxial Compressive Loadings", *Ph. D. Dissertation*, Dept. of Civil Engineering and Engineering Mechanics, University of Arizona, Tucson, AZ.

SCHOFIELD, A.N. and WROTH, C.P. (1986), *Critical State Soil Mechanics*, McGraw-Hill, London.

YUDHBIR and VARADARAJAN, A., (1975), "Stress-Path Dependent Deformation Modulus of Clay", *J. of Geotech. Engg. Div., ASCE*, Vol. 101, GT3, pp. 315-327.

### List of Nations

$a$	hardening material constant
$d\epsilon_{11}^p$	increment of normal plastic strain in the direction 11
$d\epsilon_{p_{ij}}^p$	increment of plastic strain tensor
$d\epsilon_v^p$	increment of volumetric plastic strain
$E$	Young's modulus
$F$	yield function
$\bar{F}$	modified yield function to include nonassociative behaviour
$\bar{F}_b$	component function
$F_s$	shape function
$J_1$	first stress invariant
$J_{2D}$	second invariant of deviatoric stress tensor
$J_{3D}$	third invariant of deviatoric stress tensor
$k$	nonassociative material constant
$m$	ultimate material constant
$n$	phase change material constant
$Q$	plastic potential function
$r$	$= (\sqrt{J_{2D}}) C / (\sqrt{J_{2D}}) E$
$r^*$	$= (r^4 - 1) / (r^4 + 1)$
$r_v$	$= \xi_v / \xi$
$S_{1j}$	deviatoric stress tensor
$S_r$	stress ratio $= J_{3D}^{1/3} / J_{2D}^{1/2}$
$\alpha$	growth function
$\alpha_0$	normalising constant for $\alpha$
$\alpha_1$	growth function for initial hydrostatic compression

$\alpha_Q$	growth function to include nonassociative behaviour
$\beta$	ultimate material constant
$\beta_0$	normalising constant for $\beta_1$
$\beta_1$	ultimate material constant
$\gamma$	ultimate material constant
$\lambda$	a non negative scalar factor
$\mu$	Poisson's ratio
$\xi$	trajectory of total plastic strain = $(d\epsilon_{ij}^p d\epsilon_{ij}^p)^{1/2}$
$\xi_v$	trajectory of total volumetric plastic strain
$\eta_1$	hardening material constant
$\sigma_1$	confining pressure
$\sigma_1, \sigma_2, \sigma_3$	major, intermediate and minor principal stress
$\sigma_{ij}$	total stress tensor
$\epsilon_p^{11}$	total normal plastic strain in direction 11
$\epsilon_1$	total axial plastic strain
$\epsilon_v^p$	total volumetric plastic strain